Chinese Chemical Letters 36 (2025) 109716

Contents lists available at ScienceDirect

Chinese Chemical Letters

journal homepage: www.elsevier.com/locate/cclet

Room-temperature olefin epoxidation reaction by two 2D cobalt metal-organic complexes under O_2 atmosphere: Coordination and structural regulation

Yu-Yao Li[1], Xiao-Hui Li[1], Zhi-Xuan An, Yang Chu, Xiu-Li Wang*

College of Chemistry and Materials Engineering, Professional Technology Innovation Center of Liaoning Province for Conversion Materials of Solar Cell, Bohai University, Jinzhou 121013, China

ARTICLE INFO

Article history:
Received 24 January 2024
Revised 14 February 2024
Accepted 1 March 2024
Available online 9 March 2024

Keywords:
Epoxidation
Room-temperature reaction
Metal-organic complex
Heterogeneous catalysts
Coordination unsaturated Co

ABSTRACT

Selective oxidation of olefin to epoxides is an important reaction in industry, however, developing heterogeneous catalysts to achieve the effective catalysis for this reaction under O_2 atmosphere at room temperature is challenging but highly desired. In this work, two novel 2D cobalt metal-organic complexes, namely $[Co(L)(5\text{-HIP})]\cdot 2H_2O$ (**Co-MOC-1**) and $[Co(L)(BTEC)_{0.5}]\cdot H_2O$ (**Co-MOC-2**) (L = (*E*)-4,4′-(ethene-1,2-diyl)bis(*N*-(pyridin-3-yl)benzamide; 5-H_2HIP = 5-hydroxyisophthalic acid; H_4BTEC = pyromellitic acid) were designed and synthesized through hydrothermal method, which exhibited different metal coordination modes (4-coordinate and 5-coordinate, respectively) and 2D layer structures directed by different carboxylates co-ligands. Two Co-MOCs can serve as heterogeneous catalysts for the selective oxidation of olefins to epoxides at room temperature using O_2 as oxidant. Furthermore, a higher catalysis activity of **Co-MOC-1** than **Co-MOC-2** (96.7% *vs.* 90.2% yield of 1,2-epoxycyclooctane) was observed, which may be attributed to the coordination unsaturated Co centers, the less coordination number and larger interlayer spacing of **Co-MOC-1**.

The epoxidation of olefins is one of the most important oxidation reactions [1–3], which provides valuable chemical intermediates for the production of pharmaceuticals, pharmaceutical intermediates, food additives, perfumes and agricultural chemicals [4]. Traditionally, epoxides are produced through non-catalytic processes using chlorine as oxidant or catalytic processes using peroxides as oxidants [5]. Unfortunately, these processes are uneconomical and environmentally unfriendly [6]. Green mild oxidants including air and O_2 have attracted great interest for industry and academia from both environmental and economic perspectives [7–9]. Over the past few decades, various new catalysts have been developed to achieve efficient conversion from olefins to epoxides, including homogeneous catalysts [10–13] and heterogeneous catalysts [14–17]. As is known, the homogeneous catalysts are difficult to be separated from the reaction system after reactions, which limited their application. Some heterogeneous catalysts such as MoOx NPs; $[\alpha\text{-B-SbW}_9O_{33}(t\text{BuSiO})_3\text{Ti(OiPr)}]^{3-}$ and Mo_{132} have been used for olefin epoxidation and exhibit unique advantages including easy recovery, high recyclability and stability [14–16]. However, efficient reaction under air or O_2 at room temperature is still difficult but highly desirable [18].

Metal-organic complexes (MOCs) consisting of metal ions and multiple organic ligands have become a fascinating class of heterogeneous catalysts for various organic conversion reactions [19–21]. For epoxidation reaction of olefins, some MOCs or their derived materials have been exploited [22–24]. For example, Jia's group reported PMo_{12}@UiO-67 nanocomplexes [22] and Yu's group reported CoPMA@Uio-bpy composites [23] catalysts for olefin epoxidation reaction with peroxides as oxidants. Wang's group reported a Co(II)@Cr-MIL-101-P21 catalyst, which can be used as an effective catalyst for olefin epoxidation with O_2 as oxidants at room temperature [24]. However, these heterogeneous catalysts need to introduce additionally active components into the pores of 3D MOCs to demonstrate better catalytic activity, accompanied with the problems of complicated catalyst synthesis process and easy loss of active components [25]. Pure 3D MOCs require harsh reaction conditions to achieve better catalytic effects [26]. For instance, Lin's group reported a 3D Co-MOC as catalyst for the epoxidation of olefin, but requires H_2O_2 as oxidant and longer reaction time [27].

Usually, coordination unsaturated metal centers in MOCs act as catalytic active sites for various oxidation reactions [28–30]. How-

* Corresponding author.
E-mail addresses: 925091198@qq.com, wangxiuli@bhu.edu.cn (X.-L. Wang).
[1] These authors contributed equally to this work.

https://doi.org/10.1016/j.cclet.2024.109716
1001-8417/

ever, the restraint of substrate transport and less exposed sites on the surface of large bulk 3D MOCs limit the exertion of their catalytic activity [31]. In the recent works, it is found that 2D MOCs possess superior catalytic effects than 3D MOCs due to their easier accessible catalytic sites in 2D MOCs [32,33]. Yang's team reported a 2D Cu-MOC exhibiting high catalytic effects on the synthesis of *N*-heterocyclic compounds [32]. Wang's group found that a 2D binuclear vanadium cluster-based Ni-MOC showed better catalytic effect for the selective oxidation of sulfides compared with 3D MOC [33]. Therefore, the construction of 2D MOCs with low metal coordination sites may be a promising way to achieving high-efficient catalysis for olefin epoxidation reaction at room temperature under O_2 atmosphere.

In this work, we designed and synthesized two novel 2D MOCs with different metal coordination numbers and topological structures through ligand regulation. Co ion was selected as the metal center to coordinate with a rigid dipyridine-diamide ligand L ((*E*)−4,4′-(ethene-1,2-diyl)bis(*N*-(pyridin-3-yl)benzamide), owing to the outstanding catalysis activity of Co(II) in most oxidation processes [34–36]. And two multidentate carboxylic acids (5-H_2HIP = 5-hydroxyisophthalic acid; H_4BTEC = pyromellitic acid) were used as co-ligands to regulate the structures, respectively. Two novel 2D Co-MOCs ([Co(L)(5-HIP)]·2H_2O named as **Co-MOC-1**; [Co(L)(BTEC)$_{0.5}$]·H_2O named as **Co-MOC-2**) were successfully constructed by one-pot assembly method under hydrothermal conditions. **Co-MOC-1** and **Co-MOC-2** exhibit different Co coordination (4-coordinate for **Co-MOC-1**, 5-coordinate for **Co-MOC-2**) and topological structures due to different coordination orientation of bidentate and tetradentate carboxylates. The two complexes can be used as highly efficient heterogeneous catalysts for the synthesis of epoxides at room temperature with O_2 as oxidant. Moreover, a better catalytic effect of **Co-MOC-1** than **Co-MOC-2** was found, which may be attributed to fewer coordination numbers and larger layer spacing of **Co-MOC-1**.

Synthesis of **Co-MOC-1**: Co(NO_3)$_2$·6H_2O (0.048 g, 0.15 mmol), L (0.021 g, 0.05 mmol), 5-H_2HIP (0.032 g, 0.2 mmol) and 6 mL deionized water were added to a polytetrafluoroethylene lined autoclave. The mixture was stirred at room temperature for 20 min. Then 4 mL 0.1 mol/L NaOH aqueous solution was added into the mixture and continuously stirred for 20 min. Then the mixture was sealed and heated at 160 °C for 4 days. After cooling to room temperature, purple flake crystals formed. Based on the amount of raw materials and the formula of **Co-MOC-1**, the theoretical yield of **Co-MOC-1** is calculated to be 35 mg, the actual yield of **Co-MOC-1** is 12 mg, and the yield is 33% (based on L). Element Anal. Calcd. for $C_{34}H_{28}N_4$: C, 57.81; H, 4.06; N, 8.06(%). Found: C, 57.89; H, 4.09; N, 8.12(%). Infrared data (KBr, cm^{-1}): 3569 (w), 1657 (w), 1611 (m), 1545 (s), 1486 (m), 1424 (s), 1373 (m), 1286 (s), 1191 (w), 971 (w), 897 (w), 784 (m), 691 (s), 588 (w).

Synthesis of **Co-MOC-2**: The synthesis process of **Co-MOC-2** was similar to that of **Co-MOC-1**, except that Co(NO_3)$_2$·6H_2O (0.060 g, 0.2 mmol), L (0.042 g, 0.1 mmol), H_4BTEC (0.045 g, 0.18 mmol) and 12 mL of deionized water were used. Purple flake crystals of **Co-MOC-2** were collected. Based on the amount of raw materials and the formula of **Co-MOC-2**, the theoretical yield of **Co-MOC-2** is calculated to be 62 mg, the actual yield of **Co-MOC-2** is 25 mg, and the yield is 40% (based on L). Element Anal. Calcd. for $C_{31}H_{21}N_4$: C, 60.01; H, 3.41; N, 9.03(%). Found: C, 60.07; H, 3.45; N, 9.08(%). Infrared data (KBr, cm^{-1}) 3569 (w), 3071 (w), 1667 (w), 1605 (m), 1533 (s), 1486 (s), 1420 (s), 1375 (s), 1333 (m), 1284 (s), 1191 (m), 1113 (w), 1060 (w), 963 (m), 811 (s), 765 (s), 699 (s), 584 (m), 522 (m).

Co-MOC-1 and **Co-MOC-2** crystals with the appropriate size and desired morphology were selected under an optical microscope. Data collection of **Co-MOC-1** and **Co-MOC-2** were performed on a Bruker Smart APEX II diffractometer with Mo-Kα ($\lambda = 0.71073$ Å) by the θ and ω scan mode. The structure was solved using direct methods and refined by full-matrix least-squares methods on F^2 using the Olex-2 software [37]. Crystal data and structural improvements were shown in Table S1 (Supporting information, CCDC 2310304–2310305). Selected bond lengths and angles for **Co-MOC-1** and **Co-MOC-2** were shown in Tables S2 and S3 (Supporting information).

In a typical experiment, 1 mmol cyclooctene, 10 mg catalyst, 50 mg internal standard (naphthalene), 5 mL solvent, and 2 mmol isobutyraldehyde were added to the reaction tube in turn. Then, the reaction mixture was placed on a stirrer and stirred in an O_2 atmosphere for 4 h. The yield and selectivity of the products were monitored by GC. After the reaction, the catalyst was recovered by centrifugation, then washed with ethanol at least three times. After drying in an oven at 80 °C, the catalyst was reused in recyclability experiments. For the conducting experiments on the catalytic epoxidation of olefins with different catalysts, when the mechanical mixture of Co(NO_3)$_2$/L/5-H_2HIP was used as catalyst, the amount of each component is one-third of the total amount of catalyst.

Single crystal X-ray diffraction shows that **Co-MOC-1** belongs to the monoclinic crystal system, and the space group is $P2_{1/m}$. As shown in the structural unit of **Co-MOC-1** (Fig. 1a), Co(II) is in 4-coordination mode, where two coordination N atoms come from two L ligands and two O atoms come from two 5-HIP^{2-} carboxylic acid anions. In **Co-MOC-1**, each Co(II) ion coordinates with two 5-

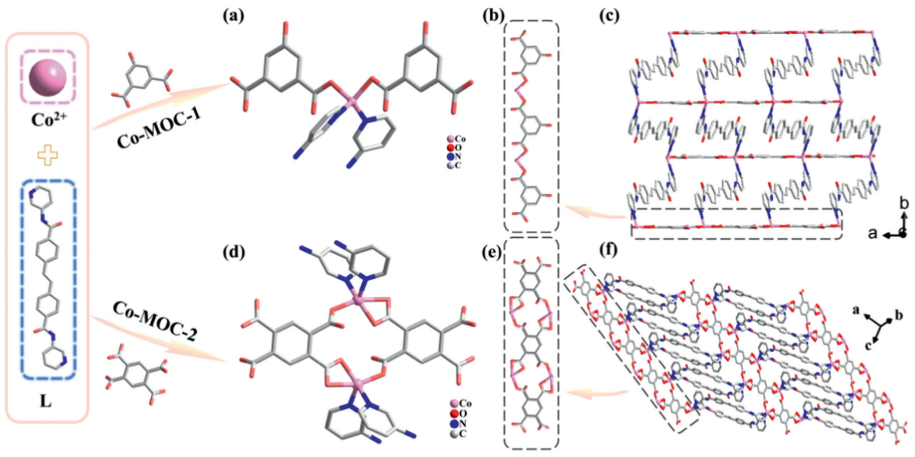

Fig. 1. The structure of **Co-MOC-1** and **Co-MOC-2**. (a, d) Coordination modes of Co centers. (b, e) 1D chain structure. (c, f) 2D layer structures.

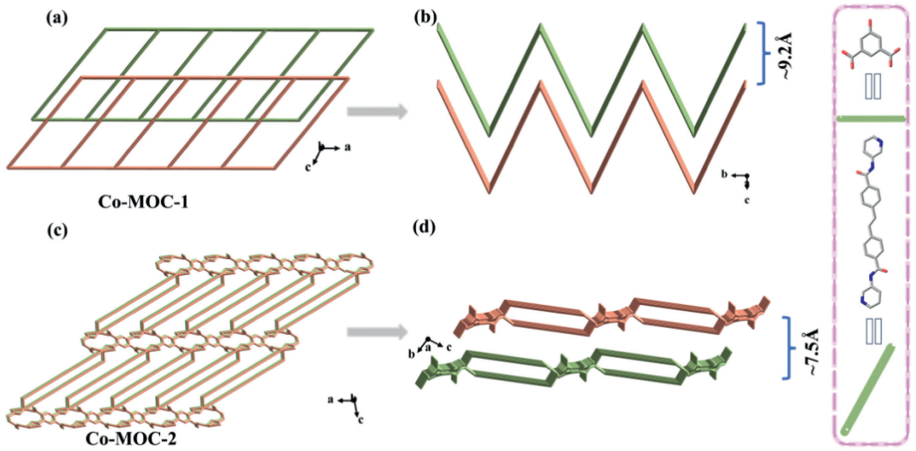

Fig. 2. (a, c) The stacked 2D layer structure diagrams of two Co-MOCs along b-axis. (b, d) The 2D layer structure diagrams and the layer spacing of two Co-MOCs along a-axis.

HIP ions to form a 1D linear $[Co(5\text{-}HIP)]_n$ chain along a-axis (Fig. 1b). The 1D $[Co(5\text{-}HIP)]_n$ chains are connected into a wavy layer in the ab plane through the coordination of Co(II) ions with L ligands (Fig. 1c and Fig. S1 in Supporting information).

Co-MOC-2 crystallizes in the P-1 space group of the triclinic system. In the metal coordination diagram of **Co-MOC-2**, Co(II) ion is 5-coordinated, consisting of two N atoms in two L ligands and three O atoms in two $BTEC^{4-}$ anions (Fig. 1d). Each $BTEC^{4-}$ anion connects four Co(II) ions to form a $[Co(BTEC)_{0.5}]_n$ ribbon chain along a-axis (Fig. 1e), and the adjacent $[Co(BTEC)_{0.5}]_n$ chains are further bridged by L ligands to form a 2D layer structure (Fig. 1f). In addition, it is shown that the 2D layers of two Co-MOCs are stacked along b-axis but exhibited different stacking modes (Figs. 2a and c). And **Co-MOC-1** shows a higher layer spacing than that of **Co-MOC-2** (9.2 Å *vs.* 7.5 Å) in Figs. 2b and d, which may endow them with different catalytic performance.

The components of **Co-MOC-1** and **Co-MOC-2** were analyzed by infrared (IR) spectroscopy (Fig. S2 in Supporting information). The peaks at 1368 and 1103 cm^{-1} in **Co-MOC-1** and 1375 and 1109 cm^{-1} in **Co-MOC-2** can be attributed to the ν(C–N) stretching vibration on the pyridine ring in the L ligand [38]. The IR absorption peaks at 1661 cm^{-1} in **Co-MOC-1** and 1667 cm^{-1} in **Co-MOC-2** belonged to the stretching vibration of the amide group [39]. The peaks at 1422 and 1613 cm^{-1} in **Co-MOC-1** and 1420 and 1605 cm^{-1} in **Co-MOC-2** were originated from the stretching vibration of the carboxyl group [40].

To determine the phase purity of the two Co-MOCs, powder X-ray diffraction (PXRD) analysis were performed (Figs. S3 and S4 in Supporting information). Except for different diffraction peak intensities, the experimental and simulated peaks of two Co-MOCs were basically consistent, indicating their good phase purity. The TG curves of **Co-MOC-1** and **Co-MOC-2** showed a similar two-step weight loss process (Figs. S5 and S6 in Supporting information). The first step of weightlessness was due to the loss of water molecules (30–365 °C for **Co-MOC-1**, 30–380 °C for **Co-MOC-2**). The second step of weight loss can be attributed to the decomposition of ligands and the collapse of the skeleton (365–500 °C for **Co-MOC-1**, 380–580 °C for **Co-MOC-2**), which indicated their excellent stability.

The catalytic performances of as-synthesized Co-MOCs for the epoxidation reaction of olefins using oxygen as the oxidant and isobutyraldehyde (IBA) as the co-reductant at room temperature were researched. Firstly, the conditions for catalytic epoxidation reaction were optimized using cyclooctene as the model substrate. As shown in Fig. 3a, **Co-MOC-1** exhibited 96.7% yield of

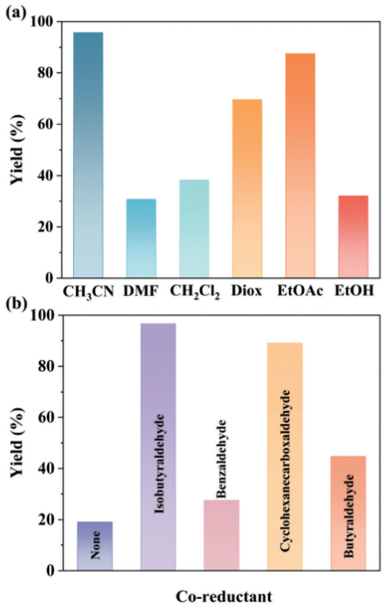

Fig. 3. (a) The effect of different solvents and (b) different aldehydes on the catalytic aerobic oxidation of cyclooctene by **Co-MOC-1**. Reaction conditions: 1 mmol of cyclooctene, 2 mmol of co-reductant, 10 mg of **Co-MOC-1** and 5 mL of solvent with O_2 balloon and react at room temperature for 4 h.

1,2-epoxycyclooctane in the solvent of acetonitrile after reaction of 4 h, while moderate yield in ethyl acetate (87.5%) and 1,4-dioxane (69.6%), and poor yield in DMF (30.7%), dichloromethane (38.3%) and ethanol (32.0%). It has been reported that aldehydes as co-reductant, play an important role in the epoxidation reaction [41]. Only 19.1% yield of 1,2-epoxycyclooctane was observed in the absence of aldehydes. Then we explored the effects of different co-reductants on the reaction in the solvent of acetonitrile. As can be seen from Fig. 3b, IBA exhibited the best promotion effect (96.7%) for the produce of 1,2-epoxycyclooctane compared with that of benzaldehyde (27.6%), butyraldehyde (44.8%) and cyclohexanecarboxaldehyde (86.1%). Finally, the effect of catalyst dosage on the epoxidation reaction was explored (Fig. S7 in Supporting information). As the increase of the catalyst dosage from 5 mg to 20 mg, the yield of 1,2-epoxycyclooctane increased first and then decreased. When the catalyst dosage was 10 mg, the yield of 1,2-epoxycyclooctane was the optimal (96.7%). The subsequent de-

Table 1
Catalytic epoxidation of cyclooctene with different catalysts.[a]

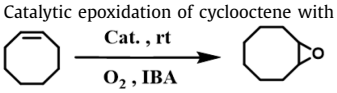

Entry	Cat.	Reaction system	Yield [b] (%)
1	**Co-MOC-1**	heterogeneous	96.7
2	**Co-MOC-2**	heterogeneous	90.2
3	3D Co-MOC	heterogeneous	86.5
4	–		26.6
5	$Co(NO_3)_2$	homogeneous	84.2
6	L	heterogeneous	33.1
7	5-H_2HIP	homogeneous	29.6
8	$Co(NO_3)_2$/L/5-H_2HIP	heterogeneous	86.4

[a] Reaction conditions: cyclooctene (0.1 mmol), CH_3CN (5 mL), IBA (2 mmol), catalyst (10 mg), room temperature, O_2 balloon, 4 h.
[b] Detect the yield of the target product 1,2-epoxycyclooctane using a GC gas chromatograph.

crease in catalytic effect may be due to the aggregation of catalyst leading to a decrease in the yield of 1,2-epoxycyclooctane [42]. When using oxygen in the air as an oxidant, the yield of 1,2-epoxycyclooctane is only 56.3%, so pure oxygen is chosen as the oxidant. At the same conditions, **Co-MOC-2** can also be used as efficient heterogeneous catalyst for epoxidation of olefin, but showed a slightly lower yield of 1,2-epoxycyclooctane (90.2%) than **Co-MOC-1** (Table 1).

In order to determine the reasons for the excellent catalytic performance of **Co-MOC-1**, a series of controlled experiments were conducted under optimal reaction conditions (Table 1). In the absence of catalyst, the yield of 1,2-epoxycyclooctane was only 26.6% (Table 1, entry 4). The raw materials of **Co-MOC-1** were used as the catalyst under optimal reaction conditions. When ligands L and 5-H_2HIP were used as catalysts, respectively, there were no significant changes from the blank reaction (33.1% and 29.6%, Table 1, entries 6 and 7). $Co(NO_3)_2{\cdot}6H_2O$ as the catalyst led to 84.2% yield of 1,2-epoxycyclooctane (Table 1, entry 5), while the mechanical mixture of $Co(NO_3)_2$/L/5-H_2HIP was used as catalyst, and the yield was similar to that of $Co(NO_3)_2{\cdot}6H_2O$ (86.4%, Table 1, entry 8). These results indicated that metal Co was the main catalytic active site in the Co-MOC frameworks.

Compared with **Co-MOC-1**, **Co-MOC-2** had different metal coordination number (4-coordinate for **CoMOC-1**, 5-coordinate for **Co-MOC-2**) and layer spacing (9.2 Å for **Co-MOC-1** and 7.5 Å for **Co-MOC-2**). A slightly lower yield by **Co-MOC-2** (90.2%) than that of **Co-MOC-1** (96.7%) was observed (Table 1, entries 1 and 2), which may be due to higher reaction possibility of Co centers in **Co-MOC-1** originated from its low metal coordination number and larger layer spacing. To further demonstrate the influence of the dimension of Co-MOCs on catalytic performances, a 3D Co-MOC, in which Co center is 5-coordinated after activation, was prepared by the self-assembly of Co(II), L ligand and 1,2,4-benzenetricarboxylic acid according to our previous work [43]. A lower yield of 86.5% was observed with the 3D Co-MOC as a catalyst compared with two 2D Co-MOCs (Table 1, entry 3). Based on the above results, it was speculated that the excellent catalytic performance of **Co-MOC-1** was probably owing to its low metal coordination and 2D layer structure with larger layer spacing leading to higher reactivity of Co active sites. Furthermore, **Co-MOC-1** had the advantages of mild reaction conditions (O_2, room temperature), shorter reaction time (4 h), and higher or similar catalytic effect compared with the catalysts reported in the literatures for epoxidation of cyclooctene due to the above advantages (Table S4 in Supporting information).

The range of substrates catalyzed by **Co-MOC-1** in the reaction system was studied under optimal reaction conditions (Table 2). For cycloalkenes such as norbornene, the catalytic effect was relatively high (yield 97.2%, Table 2, entry 2), while cyclohexene had

Table 2
Catalytic oxidation of different substrates. [a]

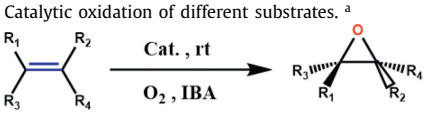

Entry	Substrate	Product	Yield [b] (%)
1			96.7
2		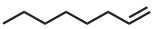	97.2
3		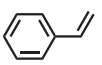	82.6
4	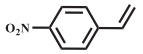	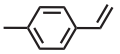	88.5
5	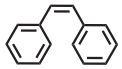		85.7
6			59.4
7	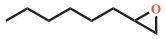	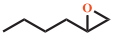	25.6
8	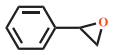	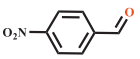	65.3
9	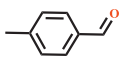	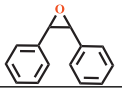	84.8

[a] Reaction conditions: substrate (0.1 mmol), CH_3CN (5 mL), IBA (2 mmol), **Co-MOC-1** (10 mg), room temperature, O_2 balloon, 4 h.
[b] Detect the yield of the target product 1,2-epoxycyclooctane using a GC gas chromatograph.

a slightly lower catalytic effect than norbornene (Table 2, entry 3, yield 82.6%). For straight-chain end-alkenes such as 1-octene and 1-hexene, corresponding epoxides can also be generated at high yield (88.5% and 85.7%) (Table 2, entries 4 and 5). For aromatic styrene, a moderate catalytic effect with a styrene oxide yield of 59.4% was observed (Table 2, entry 6). The styrene containing the electron-withdrawing group (-NO_2) was oxidized to the corresponding aldehyde, which has a very low yield (25.6%) due to its low electron density [44], and the styrene containing the electron-donating group (-CH_3) was oxidized to the corresponding aldehyde with a yield of 65.3% (Table 2, entries 7 and 8). **Co-MOC-1** also had a good catalytic effect on *cis*-stilbene with large spatial hindrance, and the corresponding epoxy product yield was 84.8% (Table 2, entry 9). These results determined that **Co-MOC-1** was a good heterogeneous catalyst for the epoxidation reaction of most olefins under mild conditions.

In order to evaluate the stability of **Co-MOC-1** catalyst in this reaction system, a thermal filtration test was conducted. After 1 h of reaction, the catalyst **Co-MOC-1** was removed by centrifugation and the remaining supernatant was allowed to continue the reaction for 3 h. As shown in Fig. 4a, removing the **Co-MOC-1** catalyst, the yield of 1,2-epoxycyclooctane increased by only 6.1% (from 49.6% to 55.7%), which should be caused by the slow oxidation of cyclooctene. **Co-MOC-1** showed high stability, which can be continuously used five times without a significant decrease in the yield of 1,2-epoxycyclooctane (from 96.7% to 93.4% in Fig. 4b). The PXRD pattern and IR spectra indicated that the structure of **Co-MOC-1** remained intact after 5 cycles (Fig. 4c and Fig. S8 in Supporting information). The XPS map of **Co-MOC-1** before and after the reaction showed that the valence state of Co does not change (Fig.

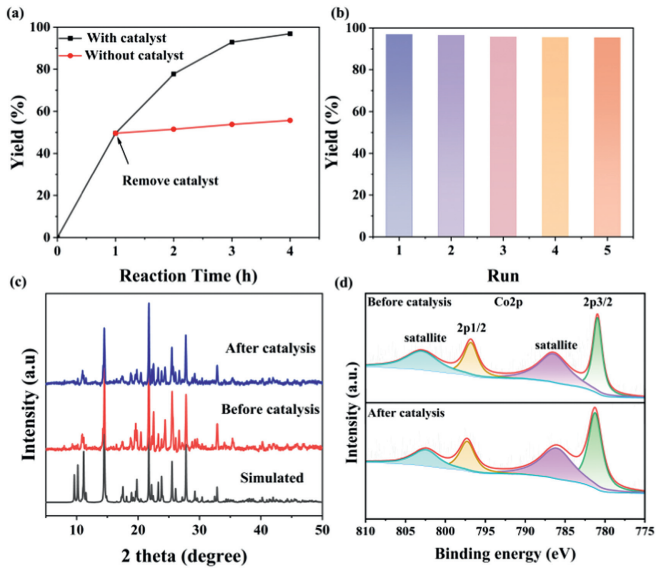

Fig. 4. (a) Hot filtration test for **Co-MOC-1**. (b) Recyclability of **Co-MOC-1** in the oxidation of cyclooctene. (c) PXRD patterns of **Co-MOC-1** before and after the catalytic reaction. (d) Co 2p XPS spectra of **Co-MOC-1** before and after the catalytic reaction.

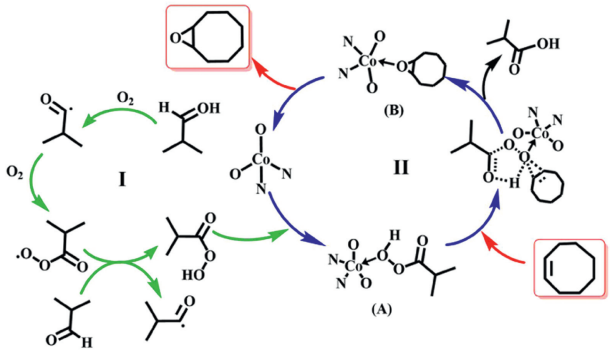

Fig. 5. Possible reaction mechanism of cyclooctene oxidation catalyzed by **Co-MOC-1**.

4d and Fig. S9 in Supporting information), which further indicates the stability of **Co-MOC-1** during the catalytic reaction process. **Co-MOC-2** also shows good heterogeneity, stability and recyclability, and can be reused five times without significant activity loss (from 90.2% to 86.4%, Figs. S10a and b in Supporting information). The PXRD pattern and IR spectra after catalytic reaction confirmed that the structure of **Co-MOC-2** remained stable (Figs. S10c and d in Supporting information).

According to the relevant literatures, oxidation reactions involving O_2 and aldehydes are generally considered to be free radical reactions [45,46]. Based on our experimental results and relevant literature [41,47], a possible reaction mechanism was proposed (Fig. 5). Firstly, IBA undergoes dehydrogenation in O_2 atmosphere to form an acyl group. Then, the acyl group continuously reacts with O_2 to form an acylperoxy radical. Afterwards, the acylperoxy radical reacts with another IBA to produce a peroxyacid and another acyl group. The peroxyacid reacts with Co-MOC catalyst to form intermediate **A**, and then the intermediate A reacts with the substrate to form intermediate **B** through the oxygen transfer step. Finally, the Co-O bond in intermediate **B** broken to form the epoxide product while the catalyst recovered.

In this article, two new 2D Co-MOCs were designed and synthesized by ligand regulation under hydrothermal conditions. Under room temperature conditions with oxygen as the oxidant, two Co-MOCs can serve as efficient heterogeneous catalysts for the epoxidation of olefins to epoxides. Within 4 h, the yield of 1,2-epoxycyclooctane catalyzed by **Co-MOC-1** was 96.7% and by **Co-MOC-2** was 90.2%. The cobalt center in Co-MOCs was proved to be an effective catalytic active site for the epoxidation of olefins. Furthermore, it was found that 2D Co-MOCs with coordination unsaturated Co centers, less metal coordination and larger layer spacing possess better catalytic performance by the comparison of **Co-MOC-1–2** reported in this work and 3D Co-MOC reported in our previous work. This work provided an effective solution for achieving catalytic oxidation reactions using molecular oxygen as an oxidant under mild conditions, which is highly desired from economical, environmental and energy perspective.

Declaration of competing interest

The authors declare no conflict of interest.

Acknowledgments

This work was financially supported by the National Natural Science Foundation of China (Nos. 22271021, 21971024, 22201021), and the Doctoral Scientific Research Foundation of Liaoning Province (No. 2022-BS-302).

Supplementary materials

Supplementary material associated with this article can be found, in the online version, at doi:10.1016/j.cclet.2024.109716.

References

[1] A. Blanckenberg, R. Malgas-Enus, Catal. Rev. 61 (2018) 27–83.
[2] N. Mizuno, K. Yamaguchi, K. Kamata, Coord. Chem. Rev. 249 (2005) 1944–1956.
[3] S.R. Waldvogel, M. Selt, Angew. Chem. Int. Ed. 55 (2016) 12578–12580.
[4] W. Zou, Y. Guo, P. Li, M. Liu, L. Hou, ChemCatChem 13 (2020) 416–424.
[5] A. Ramirez, J.L. Hueso, H. Suarez, et al., Angew. Chem. Int. Ed. 55 (2016) 11158–11161.
[6] E.V. Starokon, S.E. Malykhin, M.V. Parfenov, G.M. Zhidomirov, A.S. Kharitonov, Mol. Catal. 443 (2017) 43–51.
[7] Y. Huang, Z. Liu, G. Gao, et al., ACS Catal. 7 (2017) 4975–4985.
[8] X. Yang, Z. Liu, B. Gao, et al., ACS Catal. 13 (2023) 15572–15580.
[9] K. Schröder, B. Join, A.J. Amali, et al., Angew. Chem. Int. Ed. 50 (2011) 1425–1429.
[10] D. Zhao, J. Zhao, S. Zhao, L. He, W. Wang, Chin. Sci. Bull. 52 (2007) 2337–2344.
[11] C.J. Li, Green Chem. 4 (2002) 1–4.
[12] G. Jiang, J. Chen, H.Y. Thu, et al., Angew. Chem. Int. Ed. 47 (2008) 6638–6642.
[13] Y. Yang, F. Diederich, J.S. Valentine, J. Am. Chem. Soc. 113 (2002) 7195–7205.
[14] Y. Kuwahara, N. Furuichi, H. Seki, H. Yamashita, J. Mater. Chem. A 5 (2017) 18518–18526.
[15] A. Solé-Daura, T. Zhang, H. Fouilloux, et al., ACS Catal. 10 (2020) 4737–4750.
[16] A. Rezaeifard, R. Haddad, M. Jafarpour, M. Hakimi, J. Am. Chem. Soc. 135 (2013) 10036–10039.
[17] M. Shokouhimehr, Y. Piao, J. Kim, Y. Jang, T. Hyeon, Angew. Chem. Int. Ed. 46 (2007) 7039–7043.
[18] A.S. Sharma, V.S. Sharma, H. Kaur, R.S. Varma, Green Chem. 22 (2020) 5902–5936.
[19] J.Y. Sun, Z.L. Wang, Z. Zhang, G.C. Liu, X.L. Wang, Polyoxometalates 3 (2024) 9140039–9140044.
[20] L. Yang, Z. Zhang, C.N. Zhang, X.L. Wang, Rare Metals 43 (2024) 236–246.
[21] S. Zhang, B. Wang, S. Li, et al., J. Mol. Struct. 1297 (2024) 136929.
[22] Q. An, W. Shang, Y. Wang, et al., Inorg. Chem. Commun. 148 (2023) 110279–110284.
[23] X. Song, D. Hu, X. Yang, et al., ACS Sustain. Chem. Engin. 7 (2019) 3624–3631.
[24] J. Wang, M. Yang, W. Dong, et al., Catal. Sci. Technol. 6 (2016) 161–168.
[25] P. Lignier, M. Comotti, F. Schüth, J.L. Rousset, V. Caps, Catal. Today 141 (2009) 355–360.
[26] D. Shi, Y. Ren, H. Jiang, B. Cai, J. Lu, Inorg. Chem. 51 (2012) 6498–6506.
[27] R. Sen, D. Saha, D. Mal, P. Brandão, Z. Lin, Eur. J. Inorg. Chem. 2013 (2013) 5103–5109.
[28] N. Li, Y. Zhu, F. Jiao, et al., Nat. Commun. 13 (2022) 2742–2749.
[29] L.Y. Ustynyuk, D.V. Besedin, I.E. Nifant'ev, et al., Moscow Univ. Chem. Bull. 64 (2010) 343–365.
[30] F. Li, Q. Tang, Phys. Chem. Chem. Phys. 21 (2019) 20144–20150.
[31] S. Chang, H. An, Y. Chen, et al., ACS Appl. Mater. Interfaces 11 (2019) 37908–37919.
[32] K. Li, Y.F. Liu, X.L. Lin, G.P. Yang, Inorg. Chem. 61 (2022) 6934–6942.

[33] X. Wang, T. Zhang, Y. Li, et al., Inorg. Chem. 59 (2020) 17583–17590.
[34] S. Prakash, K. Muralirajan, C.H. Cheng, Angew. Chem. Int. Ed. 55 (2016) 1844–1848.
[35] Y. Chen, H. Shi, C.S. Lee, et al., J. Am. Chem. Soc. 143 (2021) 14445–14450.
[36] J. Werth, K. Berger, C. Uyeda, Adv. Synth. Catal. 362 (2019) 348–352.
[37] G.M. Sheldrick, Acta Crystallogr. A 64 (2008) 112–122.
[38] B. Dolenský, R. Konvalinka, M. Jakubek, V. Král, J. Mol. Struct. 1035 (2013) 124–128.
[39] J. Geng, Y. Li, H. Lin, et al., Dalton Trans. 51 (2022) 11390–11396.
[40] A. Helal, M. Fettouhi, M.E. Arafat, M.Y. Khan, M.A. Sanhoob, J. CO_2 Util. 50 (2021) 101603–101608.
[41] J. Tang, M. Cai, G. Xie, et al., Chem. Eur. J 26 (2020) 4333–4340.
[42] W. Subramonian, T.Y. Wu, S.P. Chai, J. Environ. Manage 187 (2017) 298–310.
[43] Y.Y. Li, X.H. Li, N. Xu, et al., Mol. Catal. 548 (2023) 113428.
[44] R. Li, X. Li, D. Ramella, Y. Zhao, Y. Luan, New J. Chem. 46 (2022) 5839–5847.
[45] M.J. Beier, W. Kleist, M.T. Wharmby, et al., Chem. Eur. J. 18 (2012) 887–898.
[46] Y. Li, X. Zhou, S. Chen, et al., RSC Adv. 5 (2015) 30014–30020.
[47] Y. Zheng, Q. Shen, Z. Li, X. Jing, C. Duan, Inorg. Chem. 61 (2022) 11156–11164.